Robust Model-Dependent Poisson Multi Bernoulli Mixture Trackers for Multistatic Sonar Networks

ERHAN ÖZER[ID] AND ALI KÖKSAL HOCAOĞLU[ID]
Department of Electronics Engineering, Gebze Technical University, Gebze, 41400 Kocaeli, Turkey

Corresponding author: Erhan Özer (erhanozer@gtu.edu.tr)

ABSTRACT This work proposes a robust tracker based on the Poisson Multi Bernoulli Mixture (PMBM) filter for multistatic sonar networks (MSNs) systems. The PMBM based trackers estimate the number of targets and provide the target information via Bernoulli and Poisson Point Processes. The PMBM based trackers handle existing tracks, undetected targets, and new births separately at each computation step by using these two processes together. In practice, the PMBM tracker aims to initiate the track as soon as possible and maintain the track continuity. Initiating track and maintaining track continuity are hard in challenging underwater environments without adapting the algorithm to changing environmental conditions. This paper uses the adaptive measurement-driven birth process and multistatic acoustic model-dependent probability of detection specifications. The adaptive measurement-driven birth process improves the robustness of the track initiation, and the multistatic acoustic model-dependent probability of detection advances the track continuity through the transition regions. These contributions to the PMBM tracker make it robust in terms of tracker performance in challenging underwater environments and acoustic transition regions where it is hard to get an accurate measurement.

INDEX TERMS Multistatic sonar networks, multistatic sonar tracker, multiple target tracking, Poisson multi Bernoulli mixture, random finite set, trajectory tracker.

I. INTRODUCTION

The ability to track underwater targets using active sonar systems has been a topic of interest for many years. It has been particularly challenging in practice due to the complex environmental conditions that reduce the effectiveness of sonar systems [1]. Detection probability is considerably reduced in these areas, affecting tracker performance negatively. The new rising concept against this complex environment is to employ multistatic sonar networks (MSNs) [2], [3].

In a multistatic operation, more than one sensor listens to the field illuminated by at least one source. In this way, the threat cannot detect the threatening platform. It is improbable to perform an evasive maneuver for the threat since it does not know the exact location of the receiver sensor [4]. Another main reason for choosing the multistatic operating concept is that the requirement for expensive active sources is less in this configuration compared to monostatic operations. Therefore multistatic operations are very cost-effective.

Although multistatic operations provide many advantages, they could be tolerably challenging in practice when

these sonar systems are exposed to dense clutter and ambient noise. These harsh conditions make underwater multi-target tracking a difficult problem for MSNs. Especially in low-frequency active sonar systems, clutter distributions indicate coherent characteristics [5].

Coraluppi suggests Multi-Hypotheses Tracking (MHT) type algorithms for MSNs [6], [7]. The MHT is a multi-scan approach and enhances the tracking quality, but the algorithm is based on data association, which can be complicated for underwater applications. Some recent MHT studies focus on enhancing the data association capability [8], [9]. As an alternative to the MHT, Random Finite Set (RFS) based trackers were recently proposed by Mahler [10]. There is a difference between the statistical inference problem MHT solves and the RFS filter methods solve. MHT aims to find distribution on data association and track label hypothesis, whereas RFS filters seek to obtain a posterior distribution jointly over the hypotheses and the state space [11]. With the help of an RFS filter approach, the posterior distribution of the target can be computed in a direct Bayesian approach. The RFS based, the Probability Hypothesis Density (PHD) algorithm and the Cardinalized Probability Hypothesis Density (CPHD) algorithms which are introduced by Mahler [12], [13], have been applied

to various underwater target tracking problems [14]–[16]. These filters do not establish track continuity, which is desirable for Multiple Target Tracking (MTT). Recently, the Poisson Multi Bernoulli Mixture (PMBM) algorithm was proposed as an alternative [17], which outperforms the PHD regarding the GOSPA metric in challenging scenarios [18]. Also, the PMBM filter algorithm can be converted into an algorithm for the trajectory estimation without changing the computational load [19]. Thus, PMBM based trackers can provide track continuity and can compute multiple trajectories [20].

This study mainly investigates the PMBM based methods for the MSNs to maintain the tracker performance especially in the challenging underwater conditions. The standard formulation of the probability hypothesis density PMBM filters assumes that the target birth intensity is known a priori which is inefficient since the target can appear anywhere in the challenging conditions. For this purpose, the PMBM based tracker performance is enhanced with adaptive measurement-driven birth process specifications. In addition, in this work, the tracker performance is improved by using a range-dependent multistatic acoustic model to prevent the decrease in tracking performance during the transition of the target in shadow zone and acoustic performance degraded areas. We propose the enhancements on the PMBM based tracker for the multiple target tracking and the multiple trajectory tracking. We name the PMBM tracker computing the multiple trajectories as 'T-PMBM' to keep the content integrity.

The rest of the paper is organized as follows. Section II discusses the fundamentals of the multistatic sonar system and gives a brief description of the PMBM filter. Section III describes the proposed algorithms. The simulation results showing the comparative performance of the proposed algorithms with existing algorithms are given in Section IV. Lastly, Section V concludes the article.

II. BACKGROUND

A. MULTISTATIC SONAR SYSTEM

In this section, we provide an overview of multistatic sonar systems. Accordingly, the concept of a multistatic sonar system is discussed briefly.

We can define the operating modes of modern sonar systems in three different configurations: monostatic, bistatic, and multistatic. The main difference in these operating modes is the placement of the transmitter and receiver. The receiver and transmitter are in close placement or at the same location in monostatic operations. On the other hand, in multistatic and bistatic sonar systems, the source and receiver are separated by a considerable distance. The key difference between bistatic and multistatic operation is that only one transmitter-receiver pair is available in bistatic operation, while multiple transceiver pairs are possible in multistatic operation.

The possible acoustic coverages in the case of different sonar operations are presented in Figs.1-3. It is seen from
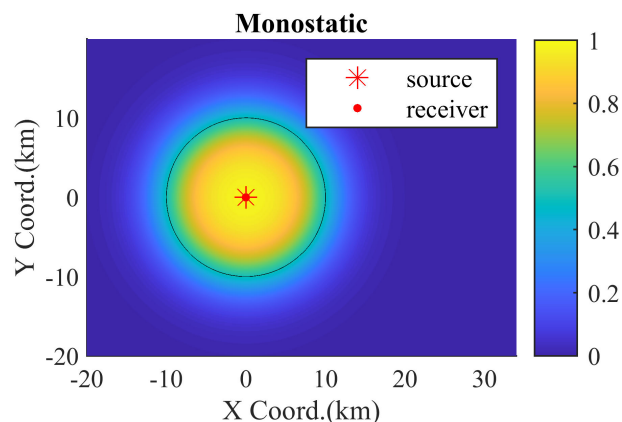

FIGURE 1. Coverage for the Monostatic Sonar Operation. The transmitter is at the same location as the receiver. Contours of the probability of detection represent the sonar coverage. The source location is shown by an asterisk, while a red dot indicates the receiver location.

FIGURE 2. Coverage for the Multistatic Sonar Operation. Contours of the probability of detection represent the sonar coverage. The source location is shown by an asterisk, while a red dot indicates the receiver location.
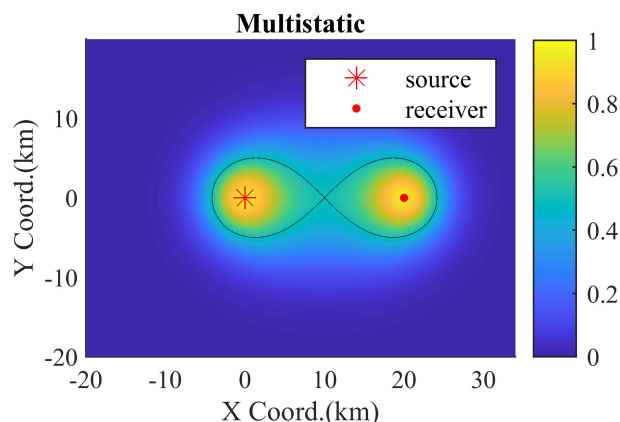
figures that in the monostatic operation that only a circular coverage area is formed around the receiver sensor (see Fig. 1), whereas, in the multistatic operation, an ellipse-like coverage is formed, which is called Cassini ovals in literature (see Fig. 2) [21].

We call the combination of these two modes as the *combined mode*. This mode has a much higher coverage rate than other modes (see Fig. 3). In the *combined mode*, the receiver process all incoming echoes.

B. THE PMBM FILTER

The PMBM filter (PMBM tracker) is an RFS-based filter approach representing the states of multiple targets over the union of a Poisson Point Process (PPP) and a Mixture of Multi Bernoulli (MBM) Process [17]. The filter applies prediction, update, and state estimation steps recursively using PPP and MBM processes. The filtering algorithm finds the
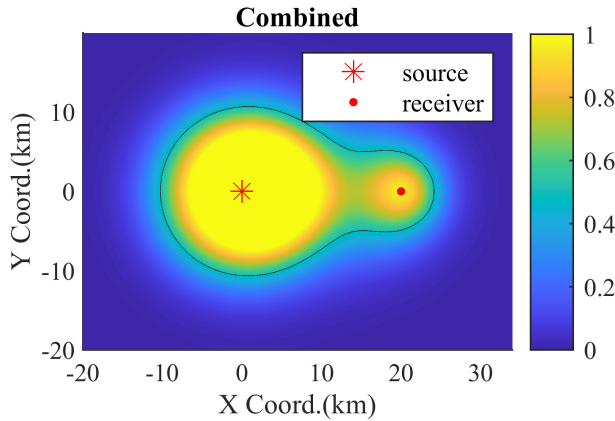
FIGURE 3. Coverage for the Combined Mode. The probability of detections of monostatic and multistatic are fused in this mode. Contours of the probability of detection represent the sonar coverage. The source location is shown by an asterisk, while a red dot indicates the receiver location.

multi-target posterior distribution of this process given the observed noisy sonar measurements in a way similar to other RFS tracking methods [22].

The disjoint union of undetected target density and detected target density processes express the multi-target density as [17], [23],

$$f_{k|k'}(\mathbf{X}) = \sum_{\mathbf{X}^u \uplus \mathbf{X}^d = \mathbf{X}} f_{k|k'}^u(\mathbf{X}^u) f_{k|k'}^d(\mathbf{X}^d) \quad (1)$$

where the undetected target has the PPP density with intensity $\lambda_{k|k'}^u(X)$,

$$f_{k|k'}^u(\mathbf{X}^u) = e^{-\int \lambda_{k|k'}^u(X)dx} \prod_{X \in \mathbf{X}^u} \lambda_{k|k'}(X), \quad (2)$$

and the linear combination of the detected target distribution has the MBM density,

$$f_{k|k'}^d(\mathbf{X}^d) \propto \sum_{a \in \mathbb{A}_{k|k'}} \omega_{k|k'}^a \sum_{\uplus \mathbf{X}^i = \mathbf{X}^d} \prod_{i \in \mathbb{T}_{k|k'}} f_{k|k'}^{i,a^i}(\mathbf{X}^i). \quad (3)$$

Here, a indicates a possible global data association hypothesis within the global data association hypotheses set, $a \in \mathbb{A}_{k|k'}$ and i is one of the tracks within the track table, $i \in \mathbb{T}_{k|k'}$. Therefore, a^i denotes hypothesis a for the track i. The weight of the global data hypothesis ($\omega_{k|k'}^a$) is a combination of weights of single hypotheses, $\omega_{k|k'}^{i,a^i}$,

$$\omega_{k|k'}^a = \prod_{i \in \mathbb{T}_{k|k'}} \omega_{k|k'}^{i,a^i}. \quad (4)$$

Considering each Multi Bernoulli component can be expressed with two parameters which are Bernoulli density ($f_{k|k'}^{i,a^i}$) and probability of existence ($r_{k|k'}^{i,a^i}$), the PMBM density (1) consists of the following parameters [19]:

$$\lambda_{k|k'}^u(\cdot), \left\{ \left(\omega_{k|k'}^{i,a^i}, r_{k|k'}^{i,a^i}, f_{k|k'}^{i,a^i}(\cdot) \right) \right\}_{a \in \mathbb{A}_{k|k'}, i \in \mathbb{T}_{k|k'}} \quad (5)$$

1) THE PMBM PREDICTION

The predicted distribution for the next step is in the form of PMBM, so the prediction step incorporates the MBM and PPP processes. Here, the PPP component follows the PHD prediction steps [12].

If the measurements fall inside a gate of predicted PPP states, new Bernoulli components are added. Simultaneously, a new target is added to the global data association hypotheses set and is considered a new potentially detected target.

The probability of survival, P^S, is another important parameter in the prediction step since this parameter directly affects the death time of existing tracks. Therefore, the survival probability plays a critical role for *previously detected tracks* and *undetected tracks*, which are implicitly kept in the algorithm.

PPP component is expressed as,

$$\lambda_{k|k'}^u(X) = \lambda_k^B(X) + \int f_{k|k'}(X|X')P^s(X')\lambda_{k'|k'}(X')dX'. \quad (6)$$

This equation can be expressed using constant P^S with a Gaussian mixture as [23],

$$\lambda_{k|k'}^u(X) = \sum_{i=1}^{N_b} \omega^{b,i} f_{k|k}^b(X) + P^s \sum_{i=1}^{N_u} \omega_{k'|k'}^{u,i} f_{k'|k'}^{u,i}(X). \quad (7)$$

The previously detected targets follow the MBM prediction steps. Equations for the transition model and prediction step are given in [10], [17] as follows:

$$f_{k|k'}^{i,a^i}(X) = \frac{\int f_{k|k'}(X|X')P_{k'}^s(X')f_{k'|k'}^{i,a^i}(X')dX'}{\langle f_{k'|k'}^{i,a^i}; P_{k'}^s \rangle}, \forall i, a^i, \quad (8)$$

$$r_{k|k'}^{i,a^i} = r_{k'|k'}^{i,a^i} \langle f_{k'|k'}^{i,a^i}; P_{k'}^s \rangle, \forall i, a^i, \quad (9)$$

$$\omega_{k|k'}^{i,a^i} = \omega_{k'|k'}^{i,a^i}, \forall i, a^i, \quad (10)$$

where $\langle f; g \rangle = \int f(x)g(x)dx$ denotes the inner product.

2) THE PMBM UPDATE

After the prediction step, the PMBM update for the standard point object model is applied to obtain the multi-target posterior density. The PMBM update step considers three types of contact: the undetected targets, the potentially detected targets, and the existing targets. Therefore, a different equation is used in the PMBM update step depending on the types of targets; accordingly, the update step is separated into three parts [17];

- Updates for the previously undetected targets (PPP)
- Updates for the new potentially detected targets (MB Update)
- Updates for the existing targets (MB Update)

a: UPDATES FOR THE PREVIOUSLY UNDETECTED TARGETS

We consider that the surviving undetected targets remain in the same status. The prior intensity of an undetected target is updated using the probability of missed detection $(1 - P_k^D(X))$

and the predicted intensity $\lambda_{k|k'}^u(X)$. The intensity update is

$$\lambda_{k|k}^u(X) = \left(1 - P_k^D(X)\right)\lambda_{k'|k}^u(X). \qquad (11)$$

b: UPDATES FOR THE NEW POTENTIALLY DETECTED TARGETS

This update step refers to a detection that is in the sonar contact list but not associated with any MB component before. If a PPP update has resulted in a potentially new target at the previous time step, the algorithm generates a new MB, and this new MB is added to the set of global data association hypotheses for the evaluation in the next iteration.

The potentially new target might originate from clutter or a detected target for the first time. These two possibilities are considered separately. The target existence probability helps to incorporate both of these possibilities.

The first hypothesis of the potentially new target is for clutter, and can be expressed as:

$$r_{k|k}^{i,1} = 0, \qquad (12)$$

$$\omega_k^{i,1} = 1. \qquad (13)$$

The second hypothesis handles the possibilities of the new tracks (i.e., the new track commencing on measurement z_k^j), and they are defined as follows:

$$r_{k|k}^{i,2} = \frac{\langle \lambda_{k|k'}^u; g(z_k^j|\cdot)P_k^D \rangle}{\lambda^{FA}(z_k^j) + \langle \lambda_{k|k'}^u; g(z_k^j|\cdot)P_k^D \rangle}, \qquad (14)$$

$$f_{k|k}^{i,2}(X) = \frac{g(z_k^j|X)P_k^D(X)\lambda_{k|k'}^u(X)}{\langle \lambda_{k|k'}^u; g(z_k^j|\cdot)P_k^D \rangle}, \qquad (15)$$

$$\omega_k^{i,2} = \lambda^{FA}(z_k^j) + \langle \lambda_{k|k'}^u; g(z_k^j|\cdot)P_k^D \rangle. \qquad (16)$$

c: UPDATES FOR THE EXISTING TARGETS

The update step for an existing target is implemented by taking into account different association hypotheses. The algorithm classifies an existing target as detection or misdetection. These two cases are considered disjointedly.

If an existing target in the prior hypothesis is not associated with any measurement, this hypothesis is called a misdetection, and a new hypothesis is added to the set of global hypotheses. The following equations are used for the update:

$$r_{k|k}^{i,a^i} = \frac{r_{k|k'}^{i,a^i}\langle f_{k|k'}^{i,a^i}; 1 - P^D \rangle}{1 - r_{k|k'}^{i,a^i}\langle f_{k|k'}^{i,a^i}; P^D \rangle}, \qquad (17)$$

$$f_{k|k}^{i,a^i}(X) = \frac{\left(1 - P^D(X)\right)f_{k|k'}^{i,a^i}(X)}{\langle f_{k|k'}^{i,a^i}; 1 - P^D \rangle}, \qquad (18)$$

$$\omega_k^{i,a^i} = \omega_{k|k'}^{i,a^i}\left(1 - r_{k|k'}^{i,a^i}\langle f_{k|k'}^{i,a^i}; P_k^D \rangle\right). \qquad (19)$$

If the association for any measurement is with any existing target, this prior hypothesis is called an existed detection, and the following equations are used to update the parameter:

$$r_{k|k}^{i,a^i} = 1, \qquad (20)$$

$$f_{k|k}^{i,a^i}(X) = \frac{P_k^D(X)g_k(z_k^j|X)f_{k|k-1}^{i,\tilde{a}^i}(X)}{\langle f_{k|k-1}^{i,\tilde{a}^i}; g(z_k^j|\cdot)P_k^D \rangle}, \qquad (21)$$

$$\omega_{k|k}^{i,a^i} = \omega_{k|k'}^{i,\tilde{a}^i}r_{k|k'}^{i,\tilde{a}^i}\langle f_{k|k-1}^{i,\tilde{a}^i}; g(z_k^j|\cdot)P_k^D \rangle, \qquad (22)$$

where this update step uses the previous hypothesis, $\tilde{a}^i$, and measurement z_k^j to update the hypothesis weight and distribution. The algorithm indeed accepts the existence of the target and sets the probability of existence to 1.

C. TRAJECTORY ESTIMATION

The trajectory information is highly desired for Anti Submarine Warfare (ASW) applications since this helps to interpret the output of the sonar systems in dense clutter regions and distinguish between moving targets. Also, trajectory information can be used by AI-based classifiers [24].

Trajectory estimation depends on the Bayesian approach, and the posterior of Trajectories RFS is recursively computed using PMBM algorithm prediction and update step. The marginalization of Trajectory RFS can extract the current state of the target [19], [25], [26]. Each RFS trajectory consists of three parameters, [27],

$$X = (\beta, \epsilon, x_{\beta:\epsilon}), \quad \beta \leq \epsilon \leq k, \qquad (23)$$

where β and ϵ are track initiation and last update time indices, respectively. Here, $x_{\beta:\epsilon}$ denotes the sequence of states

$$x_\beta, x_{\beta+1}, \ldots, x_{\epsilon+1}, x_\epsilon. \qquad (24)$$

The PMBM distribution over trajectories is a conjugate prior for the standard models, where the point process and the Poisson birth are assumed. The PPP considers undetected trajectories.

The MBM handles data association uncertainties. Each term in the mixture corresponds to a global data association hypothesis; ergo, each MB describes the distribution of the set of trajectories of the detected objects given a specific data association hypothesis.

The posterior distribution of the trajectories is calculated using all conditional relationships between states and measurements,

$$p(x_{1:k}|z_{1:k}) \propto \left(p(x_{1:k}|z_{1:k-1})p(z_k|x_k)\right), \qquad (25)$$

which increases the algorithm's complexity. Therefore, trajectory computation could become computationally intractable for long-life targets. The Bernoulli RFS approximation is used as a solution

$$p(x_{1:k}|z_{1:k}) \simeq \left(p(x_k|z_{1:k})p(x_{k-1}|z_{1:k-1})\ldots p(x_1|z_1)\right). \qquad (26)$$

This approximation considers each state independent from previous states and calculates the state using the given measurement up to that time step. After the update step of trajectories, the trajectories until the current time step are reevaluated, and the trajectory estimate is smoothed using the previous trajectory estimate to avoid a sudden jump in display and

tracker result in a smooth display. The details of this tracker are given in [19].

This paper evaluates the performances of trackers for the variable of interest as the set of trajectories and the set of target states. We add a *T* notation to the tracker abbreviation (e.g., T-PMBM) to emphasize that the output of the tracker is *Multi-Trajectory* in order to provide an explicit distinction with *Multi-Target Trackers*.

D. HYPOTHESIS REDUCTION

After the PMBM update step, all hypotheses are reconsidered, and new hypotheses are added to the set of hypotheses. Hence, the update step results in a tremendous rise in the number of global hypotheses. This significant increase in the number of global hypotheses is the bottleneck in the necessary computations. The hypothesis Reduction step helps to reduce the complexity of the PMBM tracker. The pruning is applied to the output of the Poisson process by ignoring the components whose weight is below the threshold. For the maximum number of global hypotheses, pruning is limited with predefined parameters.

Moreover, the pruning in the Poisson process, selecting the k-best global hypothesis, is implemented in the MBM process. The number of the global hypothesis is limited to a specific number hypothesis.

The logarithmic weight value of each hypothesis is calculated and fed to an optimization algorithm such as Murty's Algorithm as the cost [28]. The weight is computed by considering each combination of measurement associations. Therefore, the computation of weights consists of all possibilities (missed detection, existing target detection, new targets, false alarms/clutter).

III. THE PROPOSED POISSON MULTI BERNOULLI MIXTURE BASED ALGORITHMS

In our PMBM tracker implementation, undetected targets and new births are handled using an adaptive measurement-driven RFS PPP, while existing targets are propagated using MBM process update rules. We call this tracker Robust PMBM (RPMBM). This algorithm is presented in Section III-A.

We propose to incorporate the multistatic acoustic model-dependent probability of detection (P^D) of the MSNs into the PMBM algorithm to enhance the track continuity. Section III-B considers the computation of probability of detection and explains how we incorporate the parameter P^D into the PMBM algorithm. This proposed algorithm is named the Robust Model-Dependent PMBM (RMDPMBM).

A. ROBUST POISSON MULTI-BERNOULLI FILTER

The dynamically changing conditions of the underwater environment bring tracking difficulties for sonar systems. Sonar systems may not initiate new tracks even if they are in the measurements.

In the PMBM filter, new targets are generated based on the intensity of undetected targets. As seen in (6), the undetected intensity depends on the surviving undetected target density

and the density of the new birth. The surviving undetected targets contribute to the new potential target with smaller intensity than the birth density. In other words, the birth model plays a critical role in delivering and maintaining a new birth. In PMBM implementations, the positions of Gaussians are assumed as a known prior, so they are constant and located at the edge of the surveillance area of the tracking sensor. However, it is not straightforward to determine the surveillance area for acoustic sensors due to their changing performance depending on environmental conditions. Therefore, locating the Gaussians in birth density at the edge of the prescribed borderline of surveillance area is not always adequate for the MSNs.

This study proposes to change the positions of Gaussians of the birth model adaptively based on the measurements [29] to provide better track continuity since the birth model without an adaptive model causes deterioration in track initiation and track continuity.

Poisson RFS models the new births with the intensity depending on the components sampled from the Gaussian Mixture Model (GMM). The component of GMM depends on the previous time step propagated measurement. The newborn target intensity can be expressed as,

$$\lambda^B(x) = \sum_{n=1}^{N_b} \omega_{b,k} \mathcal{N}(x; m_{b,k}^{z_{k-1}^{(n)}}, P_{b,k}) \tag{27}$$

where $P_{b,k}$ shows the spread of the birth intensity in the vicinity of the mean values (see step-1 in Fig. 4).

The confirmation of an underwater contact as a target depends on contact continuity. This birth model supports the principle of contact continuity by considering the new possible targets in the vicinity of the previous measurement to prevent delays in target initiation.

B. ROBUST MODEL-DEPENDENT POISSON MULTI BERNOULLI MIXTURE FILTER

As seen in the PPP and MBM update steps (11-22), the posterior distribution of multiple-target directly depends on the probability of detection, $P^D(X)$. The posterior intensity for the undetected targets would be higher in regions where detection probabilities are low and vice versa. The undetected target update will lead to a small contribution from the undetected target model on the PMBM posterior in scenarios where P^D is close to one. As a result, the number of undetected targets remains the same or increases slightly. In this case, the initiation of new potential targets depends mainly on the birth states.

On the other hand, for highly cluttered regions, if P^D is assumed low, the number of undetected targets will increase and bring an additional computational cost to target initiation. Simultaneously, this brings other disadvantages, such as an increased rate of false alarms. Thus, the selection of P^D can be interpreted as a trade-off from an application point of view. Therefore the assumption of the unity of P^D in a figure of view is not realistic and causes to reduce tracking
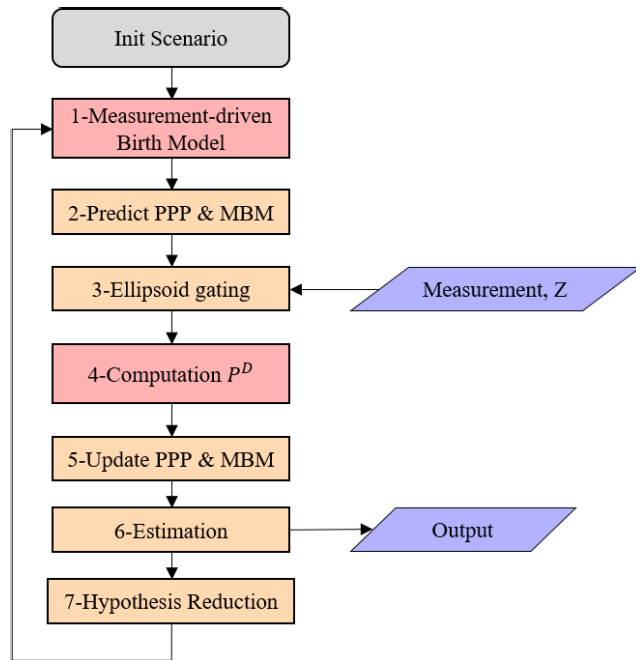
FIGURE 4. RMDPMBM algorithm flow diagram, the red nodes shows the contribution to the PMBM algorithm.

performance. Briefly, the computational accuracy of P^D is an essential parameter since this directly affects the detection reliability, which is a crucial parameter in tracking. Considering the ASW requirements, P^D should change dynamically during operation, depending on the acoustic propagation conditions [14]. Some work uses P^D as a constant term, but it is straightforward to improve the method to realistic P^D curves, such as those from the acoustic-propagation modeling. Hence, the analytical multistatic acoustic model should be preferred to compute the P^D dynamically in the multistatic operation rather than the coarse unity assumption.

The model-dependent P^D enhances tracker performance and prevents tracks in the update step from falling off the tracker in the transition regions like shadow zone or degraded acoustic performance zone. We call this model-dependent algorithm as the Robust Model-Dependent Multi Bernoulli Filter (RMDPMBM) tracker. The flow diagram of the proposed algorithm is depicted in Fig. 4. In the figure, the red nodes highlight the contribution of the proposed algorithm, while the other nodes denote the processing step of the standard PMBM filter.

The following subsection explains the computation of probability of detection for the MSNs based on Fewell's work [30].

Probability of Detection for Multistatic Sonar Networks: The tentative attempts to calculate the P^D using high-fidelity multistatic acoustic propagation modeling can be time-consuming. The expectation is that the probability of detection behaves with a decreasing trend proportional to a target range [31] due to the assumption that propagation losses are predominantly dependent on distance. The decreasing trend

of P^D can be modeled using simple models like a cookie-cutter, an exponential curve, or the Fermi function. The difference between these three approaches is the transition to the degraded acoustic detection region. The transition is smoother in the Fermi function compared to the other two curves. The Fermi function is widely used for P^D calculation, and it is given as [30],

$$P_{s,r}^D = \frac{1}{1 + 10^{(R_{multi}/R_0 - 1)/b}} \tag{28}$$

where $P_{s,r}^D$ shows a probability of detection for a single source-receiver pair. In the case of a MSN, all pairs should be considered. The b parameter shows the tail width of the Fermi function, which helps simulate the smooth transition to the shadow zone or out of the figure of merit. Here, R_0 is a range of the day concerning 50% detection probability, and R_{multi} denotes the distance for the bistatic propagation loss or equivalent monostatic range. R_{multi} is expressed with the distances source-target and target-receiver by [32] as,

$$R_{multi} = \sqrt{R_{ST} R_{TR}} \ . \tag{29}$$

Another vital issue for P^D is the limits due to signal processing. For example, detection during transmission is not feasible without pulse compression, which causes a blind zone near the receiver. In the multistatic operation, a blind zone occurs near the receiver, caused by the direct blast effect. It is not possible to detect the target echos till the direct blast arrives in the receiver. The shape of the blind zone is an ellipse, and the form is directly related to the receiver-source distance. If the following equality holds within the scenario, a blind zone occurs:

$$R_{ST} + R_{TR} < R_{SR} + 2R_b. \tag{30}$$

The acoustic propagation model considers a blind zone by hard thresholding the P^D. Thus, the P^D equals 0 for the closer distance than the blind zone, R_b. Equation (28) becomes,

$$P_{s,r}^D = \begin{cases} \dfrac{1}{1 + 10^{(R_{multi}/R_0 - 1)/b}} & \text{if } R_{multi} > R_b, \\ 0 & \text{otherwise.} \end{cases} \tag{31}$$

An acoustic model was created within the framework of a multistatic scenario, and the *Fermi* model, which is used in many academic studies on multistatic, was preferred for coverage and probability of detection modeling [30], [31], [33].

The total probability of detection for MSNs, P_t^D, is revised by taking into account the Signal Excess (SE), which shows the level of signal excess in dB above the Detection Threshold (DT) and decreases with the distance. The SE computation for the multistatic active sonar requires multiple solutions of the bistatic sonar equation, which is given in noise-limited conditions as [34],

$$\text{SE} = \text{SL} + \text{TS} - \text{TL}_{ST} - \text{TL}_{TR} - \text{NL} - \text{DT}. \tag{32}$$

Here, SL is the transmitter's source level. The target geometry and scattering characteristic is considered by the Target Strength (TS) term. Another essential term is the Noise

Level (NL). It is the interference to the sensor originating from the environment or shipping. Therefore, NL directly affects sonar performance, reducing the signal-to-noise ratio (SNR). NL is usually assumed an isotropic. The last term in the sonar equation is the Transmission Loss (TL), mainly dependent on the acoustic range-dependent spreading and absorption loss. All parameters of the sonar equation are almost consistent for a short time except TL, which is directly dependent on the target distance. TL can be expressed as [32],

$$\text{TL}_{multi} = k\log(R_{ST}R_{TR}) + \alpha(R_{ST} + R_{TR}) \tag{33}$$

where α is the attenuation coefficient, and k is the geometrical propagation loss coefficient (k is equal to, e.g., 20 for spherical spreading, 10 for cylindrical spreading). The propagation distance is equal to the sum of the source-target and target-receiver distances.

However, the spreading loss is assumed a predominated effect in TL; the absorption losses might be crucial for the model in high frequencies [1]. Thus, the absorption loss is incorporated in the acoustic model as a correction factor.

After the calculating the P^D using the Fermi function, the absorption correction is made to the P^D in line with the absorption losses regarding the transmission frequency and target range. The $\text{SE} - P^D$ transition is performed using the following equation [30]:

$$\text{SE}_{uncorr.} = \sigma_n\sqrt{2}\text{inverf}(2P^D - 1) \tag{34}$$

where the *inverf* corresponds to the inverse error function. The standard deviation of noise is set as $\sigma_n = 8$ (dB). Urick suggested this value since the usage of this value results in significant similarities to the experiment. Then, the absorption correction is applied regarding (33),

$$\text{SE}_{corr} = \text{SE}_{uncorr.} - \alpha(R_{st} + R_{rt} - 2R_{equiv}). \tag{35}$$

At last, the P^D is recalculated for each trans-receiver pair using the following transition equation:

$$P^D_{s,r} = \frac{1}{2}\left(1 + \text{erf}\left(\frac{\text{SE}}{\sigma_n\sqrt{2}}\right)\right). \tag{36}$$

Assuming all probabilities are independent and considering all trans-receiver pairs in the network, the total probability of detection for MSNs can be expressed as [31],

$$P^D_t = 1 - \prod_{(s,r)\in S\times R} 1 - P^D_{s,r} \tag{37}$$

where the source is $s \in S$, and the receiver is $r \in R$.

IV. SIMULATION AND RESULTS
A. MODEL
Under the linear Gaussian dynamics, this paper assumes a point target measurement model [35]. The following equations are used for modeling the target motion and the measurement process:

$$f_{k|k'}(x|\zeta) = \mathcal{N}(x; F_{k-1}\zeta, Q_{k-1}), \tag{38}$$

$$g_k(z|x) = \mathcal{N}(z; H_k x, R_k), \tag{39}$$

where ζ corresponds to the previous state. The tracker performs in a track-oriented fashion by assuming that each gated measurement creates a new track hypothesis.

1) THE MEASUREMENT MODEL
The measurements are obtained from the simulation of an underwater multistatic sonar network system consisting of more than one receiver and transmitter pair. The components of each measurement are the range (in meters) and the bearing (in radians). The measurement model utilizes ellipsoidal gating in order to ignore the very unlikely measurements. The measurement component can be expressed as,

$$\begin{bmatrix} \theta \\ r \end{bmatrix} = \begin{bmatrix} tan^{-1}(\frac{y - y_r}{x - x_r}) \\ t_{toa} \times sos \end{bmatrix} + \omega, \quad \omega \sim \mathcal{N}(0, \Sigma) \tag{40}$$

where t_{toa} refers to the *time of arrival* and *sos* is the *speed of sound*.

The measurement model incorporates the false contacts to the scenario by combining the clutter model measurements with the target originating measurement. The measurement model considers the clutter model as the homogeneously distributed Poisson model with a density parameter λ equals 10. Thus, the clutter model generates an average of 10 clutter measurements per transmission. False measurements are uniformly distributed through the surveillance area (6 km $\times$ 6 km).

2) THE MOTION MODEL
The motion model follows linear Gaussian dynamics with a constant survival probability, $p_{S,k} = 0.99$. A target state has the position and velocity components:

$$x_k = [p_{x,k}, \dot{p}_{x,k}, p_{y,k}, \dot{p}_{y,k}]. \tag{41}$$

In the case of trajectory tracking, the trajectory state consists of the target state, track initiation (β), and last existence time indices (ϵ) [36]. It is defined as follows:

$$X = (\beta, \epsilon, x_{\beta:\epsilon}), \quad \beta \leq \epsilon \leq k. \tag{42}$$

3) THE TARGET BIRTH MODEL
The GMM is used for the generation of the birth's prior. The position components are updated by the measurement, which is obtained at the previous time step. The velocity component is randomly sampled using the GMM, assuming that the tracker tracks solely moving targets.

The number of birth is time-varying, and it is dependent on the number of measurements. The predefined Gaussian model (with $\sigma_v = 0.5m/s^2$) is used for the velocity components of birth's prior. The covariance matrix is selected as,

$$P_b = \begin{bmatrix} 100 & 0 & 0 & 0 \\ 0 & 0.25 & 0 & 0 \\ 0 & 0 & 100 & 0 \\ 0 & 0 & 0 & 0.25 \end{bmatrix}. \tag{43}$$

4) PERFORMANCE EVALUATION

In this paper, the performance of multi-target tracking is evaluated by using the Generalized Optimal Sub-Pattern Assignment (GOSPA) metric [37].

When the parameter α equals 2, the GOSPA metric can be written as,

$$\mathbb{E}\left[d_1^{c,2}(\hat{\mathbf{x}}, \mathbf{x})\right] = \left[\min_{\gamma \in \Gamma}\left(\sum_{(i,j) \in \gamma} d(x^i, \hat{x}^j)^p \right.\right.$$
$$\left.\left. + \frac{c^p}{2}\left(|\mathbf{x}| - |\gamma| + |\hat{\mathbf{x}}| - |\gamma|\right)\right)\right]^{\frac{1}{p}} \quad (44)$$

where $d^{(c)}(x, \hat{x}) = \min(c, d(x, \hat{x}))$ refers to the distance between the position of the set of the truth (x), and the position of the set of the estimation $(\hat{x})$ with a cut-off at c. A cut-off, c, is a design variable and refers to the cost of missed and false targets. The γ denotes the correctly detected targets. The difference with γ can penalize missed and false targets, respectively, in this equation. The last parameter, p, refers to the state space's Lp norm.

B. SCENARIO AND RESULTS

We present three different scenarios to investigate the performances of the proposed PMBM and T-PMBM algorithms. Firstly, we consider a single target tracking problem for the high probability of detection rates. Then we reduce the probability of detection rates and reevaluate the tracker performance in Scenario-2. Finally, multiple-target tracking performance is considered in Scenario-3. In all scenarios, the multistatic P^D values are obtained from the Fermi function with a diffusivity of 0.5. The attenuation coefficient is $\alpha = 0.1$dB/km, an appropriate coefficient for an acoustic frequency of about 1.5 kHz [1]. The range of the day is set to 350 m. We consider six fixed sensor nodes in the MSN. The sensor nodes behave like the multistatic sonar, and their transducer has no directivity, so all transmissions are omnidirectional within the scenario. The active nodes ensonify the surveillance area. All sensor nodes (including its receiver) receive the backscattered echoes and generate the contact information. All contacts are collected and fused by a processing center. Therefore, the network-centric tracker generates a combined coverage region that is desired to enhance the coverage.

All targets act as point source target that has a constant route and speed during the scenario. We keep the ship noise interference and shallow water-oriented reverberation within the scenario by adding clutter to the measurement.

The blind zone elimination is not applied, so the acoustic model considers a blind zone in the vicinity of the receiver nodes whether it works monostatic or as a multistatic receiver. The common scenario parameters are shown in Table 1.

1) SCENARIO-1: HIGH PROBABILITY DETECTION RATE

In this scenario, a single underwater target aims to circumvent the MSN to avoid detection. We consider the densely located

TABLE 1. List of common scenario parameters.

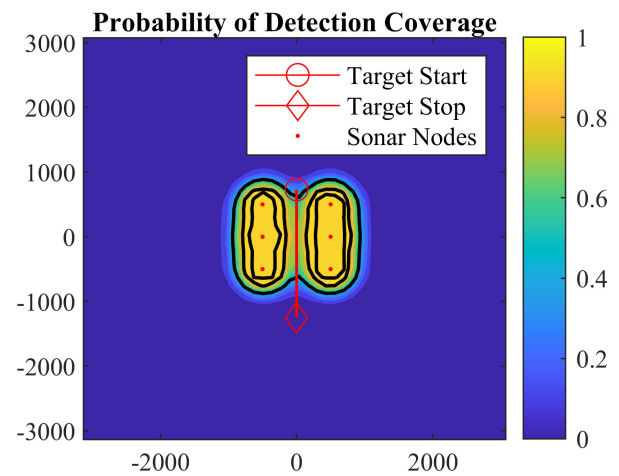|	
Number of Monte Carlo	100
Number Of Node	6
Range of Day(meter)	350
Prob. of Detection	0.90
Prob. of Survival	0.99
λ	10
Clutter Intensity	2.778e-07
Gating Val.	0.99
Pruning Threshold	0.001
Max. Hypothesis Number	100
Selected Metric	GOSPA
Metric Param. c Val.	50
Metric Param. p Val.	1
Metric Param. α Val.	2

FIGURE 5. This figure illustrates the sonar coverage of Scenario-1 for densely located six sonar nodes (red dot). The nodes are equally separated with 1000 meters in horizontal axes and 500 meters in vertical axes. Contours of the probability of detection represent the sonar coverage. The initial position of a target trajectory is marked with a red circle, while the last position is marked with a red diamond.

network nodes. It causes to reduce the coverage rate but increases the probability of detection in this limited region, shown in Fig. 5. This figure illustrates the sonar coverage of Scenario-1 for densely located six sonar nodes (red dot). The nodes are equally separated with 1000 meters in horizontal axes and 500 meters in vertical axes. The initial position of a target trajectory is marked with a red circle, while the last position is marked with a red diamond. The probability of detection of MSN is displayed with contour lines that take values between 0-1. The resulting data set consists of 100 scans with a one-second sampling interval.

The simulation results are presented in Table 2. It is observed that the algorithm with the lowest error is the proposed algorithm RMDPMBM. The most significant reason for the increase in performance is that the RMDPMBM algorithm is based on the multistatic acoustic model, which assumes that the probability of target detection in the

TABLE 2. Scenario-1, the comparison of GOSPA metric of different PMBM trackers on the multistatic sonar network simulation data set.

Tracker	Avg. Comput. Time (sec.)	Average GOSPA Cost			
		Missed	False	Position	Total
PMBM	2.58	16.36	16.73	4.06	37.15
RPMBM	2.85	10.58	10.80	6.62	28.00
RMDPMBM	8.28	4.86	5.00	11.28	21.14
T-PMBM	2.67	16.68	17.03	3.89	37.60
T-RPMBM	3.04	11.10	11.32	6.38	28.80
T-RMDPMBM	7.09	5.79	5.91	10.28	21.98

coverage areas will be low, preventing breaks in the tracking and thus ensuring the track continuity. The multistatic model-dependent trackers have a better performance in terms of false and missed target costs. However, they are not among the best tracker regarding the position error since they utilize the adaptive P_D value in computation, which might cause a rise in uncertainty near the acoustic performance transition regions.

An important consideration regarding the table is the effect of the birth model on the solution. The PMBM tracker with fixed birth model parameters does not initiate a tracker until the required criteria are met. The target initiation criteria highly depend on the birth model intensity. RPMBM and T-RPMBM trackers use the proposed adaptive birth model. The usage of the adaptive birth model increases the possibility of initiating new targets. Therefore, these algorithms initiate new targets quickly after the first measurement obtained from the target. When the fixed birth model-dependent PMBM and T-PMBM algorithms are compared with the adaptive birth model-dependent RPMBM and T-RPMBM algorithms, it is seen that algorithms with the adaptive birth model are superior. The position error of the GOSPA metric is illustrated for different trackers in Fig. 8. In this figure, some trackers have no position error at some scans, as these trackers do not have an existing track at these scans. Therefore, their GOSPA metric consists only of the cardinality error at these scans. Average GOSPA metric results for all considered trackers are depicted in Figs. 6-9.

2) SCENARIO-2: LOW PROBABILITY DETECTION RATE

This scenario aims to evaluate the performance of the MSN when the coverage rate is low. So, we increase the distance between the nodes in this scenario. This positioning approach reduces the probability of detection in the figure of merit while increasing the coverage. Therefore, some degraded acoustic zone exists between nodes which provide an escape opportunity to the adversary unit, shown in Fig. 10. The resulting data set consists of 100 scans with a one-second sampling interval.

The vital benefit of the multistatic acoustic model can be easily seen in this scenario since transition zones appear throughout the route of the target, which degrades the measurement accuracy. Consistent measurements are not
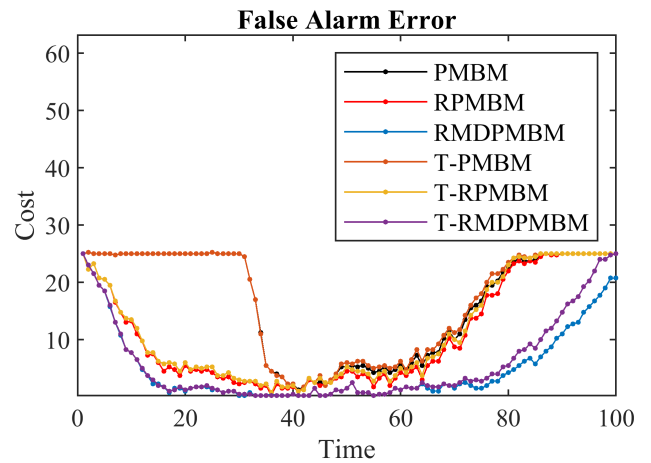

FIGURE 6. Scenario-1, the false alarm error of the average GOSPA metric for different trackers.
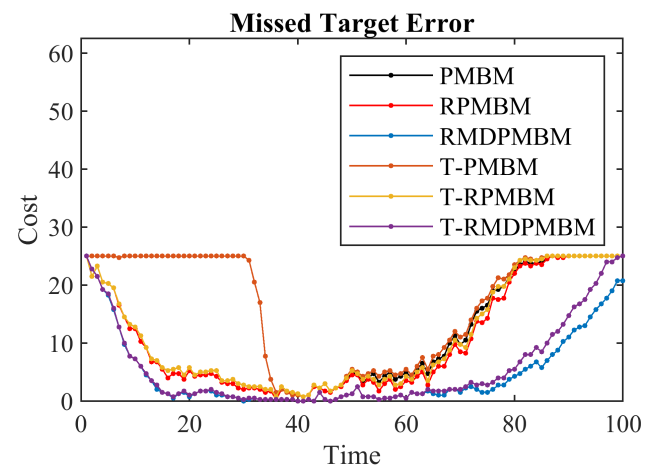

FIGURE 7. Scenario-1, the missed target error of the average GOSPA metric for different trackers.

possible in the vicinity of acoustic degraded zones. The model-dependent algorithms change the P^D value following the multistatic acoustic model. This model helps to improve track continuity. T-RMDPMBM and RMDPMBM are superior in terms of false and missed target cost. The difference in false and missed target costs is significant among the algorithms. While the positioning cost is comparable (see Table 3).

As expected, PMBM trackers show similar tracking performance characteristics in areas with high target detection probability. However, there are differences in tracking performance near 'transition zones,' where the performance of acoustic detection is reduced. The transition region causes the oscillation in tracker result, and the average GOSPA metric results illustrate this effect explicitly (see Figs. 11-14). The target passes two times through the transition zone during the scenario, and the T-RMDPMBM and RMDPMBM trackers have a better performance than other trackers at this time
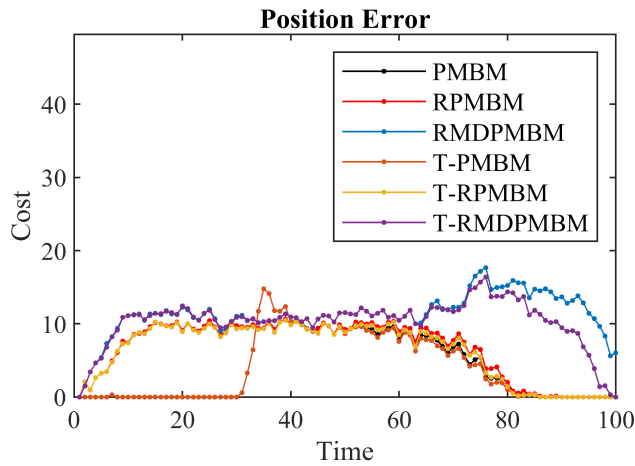
FIGURE 8. Scenario-1, the position error of the average GOSPA metric is illustrated for different trackers. Some tracker has no position error at some scans, as these trackers do not have an existing track at these scans. Therefore, their GOSPA metric consists only of the cardinality error at these scans.
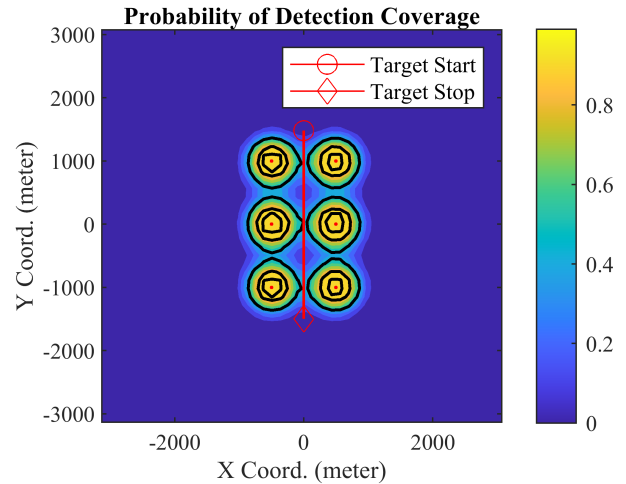

FIGURE 10. Scenario-2, Coverage for the Multistatic Sonar Network. The nodes are equally separated with a distance of 1000 meters in horizontal and vertical axes. In this scenario, the route of the target has a low probability of detection compared to Scenario-1.
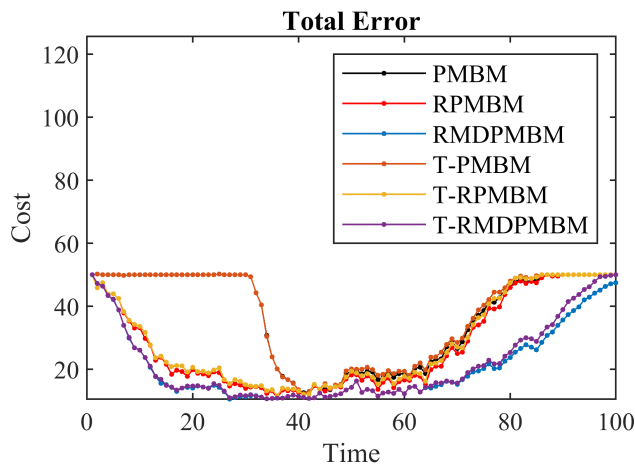
FIGURE 9. Scenario-1, the total error of the average GOSPA metric. Shown is the overall GOSPA error for all six trackers.
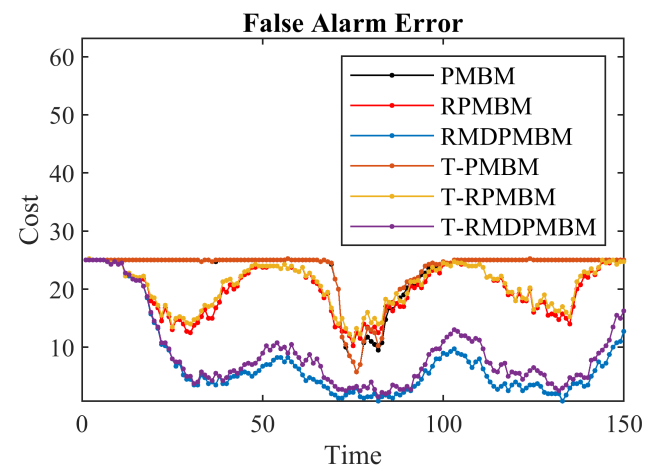

FIGURE 11. Scenario-2, the false alarm error of the average GOSPA metric for different trackers.

TABLE 3. Scenario-2, the comparison of GOSPA metric of different PMBM trackers on the multistatic sonar network simulation data set.

Tracker	Avg. Comput. Time (sec.)	Average GOSPA Cost			
		Missed	False	Position	Total
PMBM	2.81	23.13	23.20	1.03	47.36
RPMBM	3.00	19.78	19.86	3.00	42.64
RMDPMBM	14.74	7.13	7.30	11.72	26.15
T-PMBM	2.67	23.30	23.36	0.95	47.61
T-RPMBM	2.97	20.35	20.42	2.71	43.48
T-RMDPMBM	9.85	8.80	8.92	10.53	28.25

steps. It is seen that the use of fixed P^D causes a rupture in the target tracking, especially in the transition regions where the probability of detection is low. On the other hand, with the multistatic acoustic model, the changes in the transition regions cause a minimum decrease in the overall tracking performance.

3) SCENARIO-3: MULTIPLE TARGET TRACKING

In this scenario, we add three additional targets to Scenario-2. Hence, this scenario helps to evaluate multiple target tracking performance of PMBM-based algorithms. The scenario consists of 150 scans with a one-second sampling interval. The scenario is illustrated in Fig. 15, and the plot of the received contacts versus ground truth is displayed in Fig. 16. The initial position of the true trajectory is marked with a red circle, while the last position is marked with a red diamond. The running time and GOSPA metric of the six algorithms are analyzed and compared in Table 4. All trackers produce false targets because of the dense clutter. Only T-RMDPMBM and RMDPMBM trackers successfully
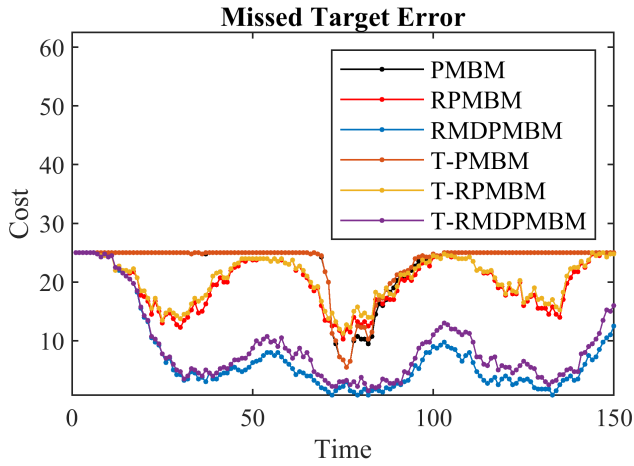
FIGURE 12. Scenario-2, the missed target error of the average GOSPA metric for different trackers.
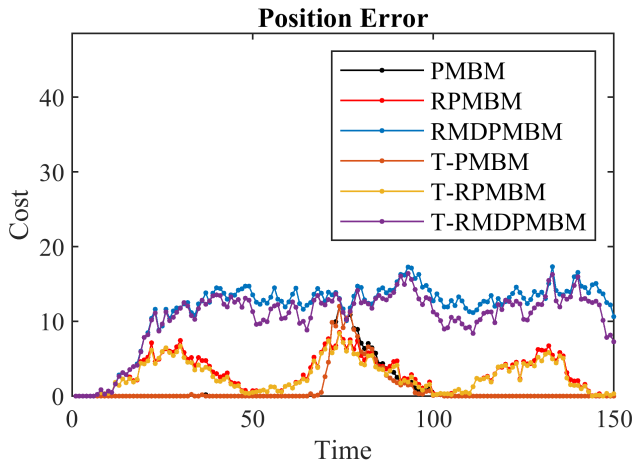

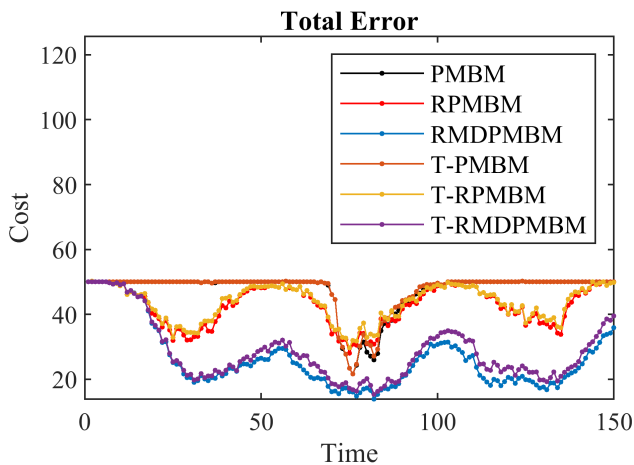**FIGURE 13.** Scenario-2, the position error of the GOSPA metric is illustrated for different trackers.

FIGURE 14. Scenario-2, the total error of the average GOSPA metric. Shown is the overall GOSPA error for all six trackers.

FIGURE 15. Scenario-3, the sonar coverage. The initial position of a true trajectory is marked with a red circle, while the last position is marked with a red diamond.
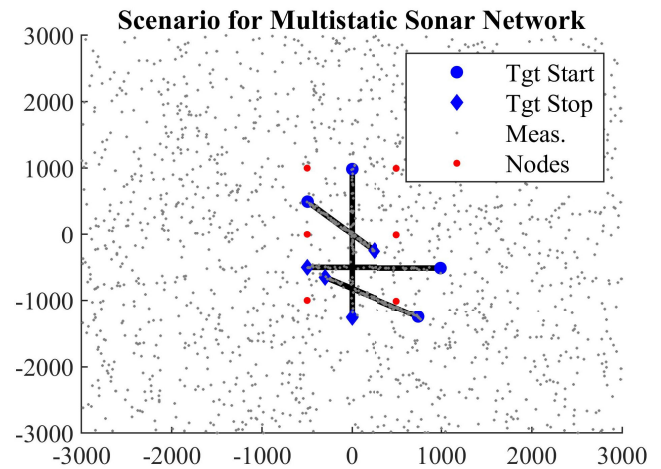
FIGURE 16. Scenario-3, the initial position of a true trajectory is marked with a blue circle, while the last position is marked with a blue diamond, and measurements are displayed with a gray-colored plus marker.

TABLE 4. Scenario-3, the comparison of GOSPA metric of different PMBM trackers on the multistatic sonar network simulation data set.

Tracker	Avg. Comput. Time (sec.)	Average GOSPA Cost			
		Missed	False	Position	Total
PMBM	3.73	89.16	15.39	5.58	110.13
RPMBM	6.35	50.81	1.84	21.62	74.27
RMDPMBM	74.20	18.55	2.87	44.78	66.20
T-PMBM	3.72	89.77	15.78	5.25	110.80
T-RPMBM	6.97	53.47	2.10	20.21	75.78
T-RMDPMBM	35.18	22.56	2.10	41.63	66.29

maintain track continuity even in the degraded region (see Figs. 17 and 18). Nevertheless, their target position error rises near the degraded region (see Fig. 19). However, the general
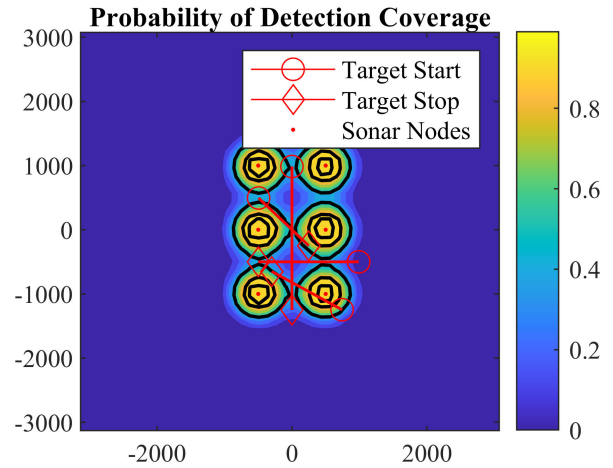
characteristics of average GOSPA metric results are quite similar to those of other scenarios. The average running time of the RMDPMBM tracker increases significantly for this scenario. The increase in time is due to the increasing number of targets because the algorithm dynamically calculates P^D
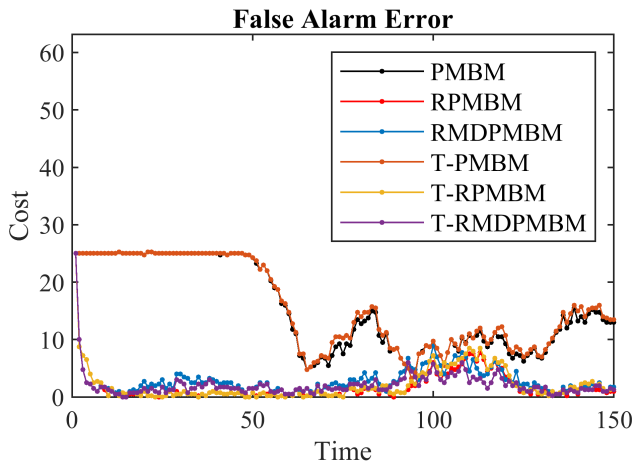
False Alarm Error

FIGURE 17. Scenario-3, the false alarm error of the average GOSPA metric for different trackers.

Missed Target Error

FIGURE 18. Scenario-3, the missed target error of the average GOSPA metric for different trackers.

Position Error

FIGURE 19. Scenario-3, the position error of the GOSPA metric is illustrated for different trackers.

for each target. A lookup table of P^D can be used for a specific region to avoid this computational burden. The PC platform is Intel(R) Xeon(R) CPU E5-2660 v3 @ 2.60GHz (2 processors), RAM 32.0 G, MATLAB R2021a. The overall
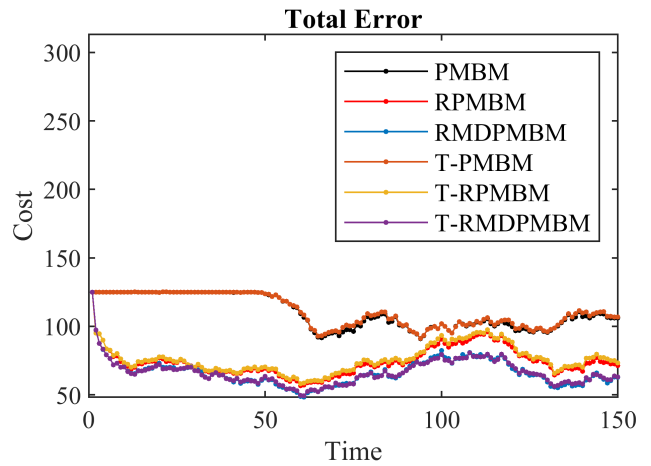
Total Error

FIGURE 20. Scenario-3, the total error of the average GOSPA metric. Shown is the overall GOSPA error for all six trackers.

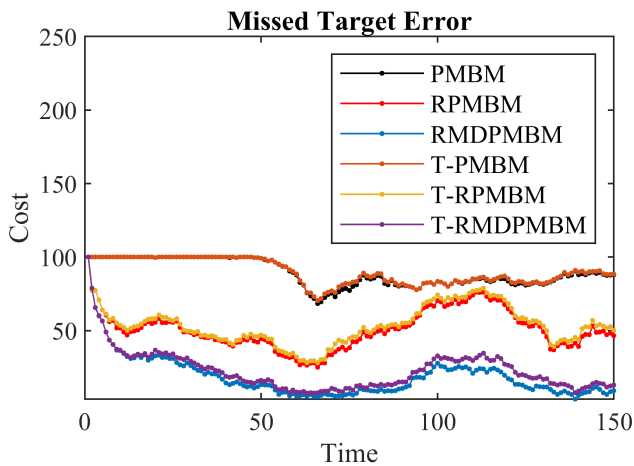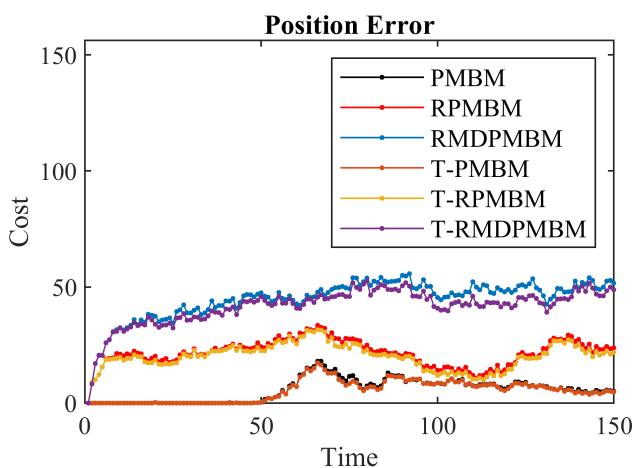performance comparison of the PMBM based trackers is illustrated in Fig. 20. It is seen from the figure that the RMDPMBM tracker performs very well during the scenario.

V. CONCLUSION

In this paper, we have proposed two extensions of the PMBM algorithm for underwater target tracking on Multistatic Sonar Networks in challenging conditions. Firstly, we use the adaptive measurement-driven Poisson Birth Model in the PMBM prediction step to achieve robustness against the changes in cardinality. The proposed robust PMBM (RPMBM) tracker improves the target initiation performance within PMBM and outperforms the priori known birth intensity model-based PMBM tracker.

Subsequently, we have enhanced the RPMBM tracker performance by involving the probability of detection, which is the multistatic model-dependent and computed within each scan for all trans-receiver pairs, in the update process. This proposed robust model-dependent PMBM (RMDPMBM) algorithm has been compared to other PMBM based trackers by the numerical simulations, and the performances of trackers are assessed for the variable of interest as the set of trajectories and the set of target states.

The simulation results show that the proposed algorithm outperforms and provides an advantage in reducing false tracks without impairing track continuity for MSNs in dense clutter regions. The principal manifestations of this improved performance are the reduction of false tracks and continuous target tracking without fragmentation.

REFERENCES

[1] R. J. Urick, *Principles of Underwater Sound*. New York, NY, USA: McGraw-Hill, 1983.

[2] S. Kim, B. Ku, W. Hong, and H. Ko, "Performance comparison of target localization for active sonar systems," *IEEE Trans. Aerosp. Electron. Syst.*, vol. 44, no. 4, pp. 1371–1380, Oct. 2008.

[3] E. Craparo and M. Karatas, "Optimal source placement for point coverage in active multistatic sonar networks," *Nav. Res. Logistics (NRL)*, vol. 67, no. 1, pp. 63–74, Feb. 2020.

[4] S. Zhou and P. Willett, "Submarine location estimation via a network of detection-only sensors," *IEEE Trans. Signal Process.*, vol. 55, no. 6, pp. 3104–3115, Jun. 2007.

[5] M. E. G. D. Colin and S. P. Beerens, "False-alarm reduction for low-frequency active sonar with BPSK pulses: Experimental results," *IEEE J. Ocean. Eng.*, vol. 36, no. 1, pp. 52–59, Jan. 2011.

[6] S. Coraluppi and C. Carthel, "Multi-hypothesis sonar tracking," in *Proc. 7th Int. Conf. Inf. Fusion*, 2004, pp. 33–40.

[7] S. Coraluppi and C. Carthel, "Distributed tracking in multistatic sonar," *IEEE Trans. Aerosp. Electron. Syst.*, vol. 41, no. 3, pp. 1138–1147, Jul. 2005.

[8] H. Shin, B. Ku, J. K. Nelson, and H. Ko, "Robust target tracking with multi-static sensors under insufficient TDOA information," *Sensors*, vol. 18, no. 5, pp. 1481–1498, May 2018. [Online]. Available: https://www.mdpi.com/1424-8220/18/5/1481

[9] Y. Yao, J. Zhao, and L. Wu, "Doppler data association scheme for multi-target tracking in an active sonar system," *Sensors*, vol. 19, no. 9, p. 2003, Apr. 2019. [Online]. Available: https://www.mdpi.com/1424-8220/19/9/2003

[10] R. Mahler, *Statistical Multisource-Multitarget Information Fusion*. Norwood, MA, USA: Artech House, Inc., 2007.

[11] M. Üney, "Type II approximate Bayes perspective to multiple hypothesis tracking," in *Proc. 22nd Int. Conf. Inf. Fusion*, Jul. 2019, pp. 1–8.

[12] R. P. S. Mahler, "Multitarget Bayes filtering via first-order multitarget moments," *IEEE Trans. Aerosp. Electron. Syst.*, vol. 39, no. 4, pp. 1152–1178, Oct. 2003.

[13] R. Mahler, "PHD filters of higher order in target number," *IEEE Trans. Aerosp. Electron. Syst.*, vol. 43, no. 4, pp. 1523–1543, Oct. 2007.

[14] R. Georgescu and P. Willett, "The GM-CPHD tracker applied to real and realistic multistatic sonar data sets," *IEEE J. Ocean. Eng.*, vol. 37, no. 2, pp. 220–235, Apr. 2012.

[15] X. Chen, Y. Li, Y. Li, and J. Yu, "PHD and CPHD algorithms based on a novel detection probability applied in an active sonar tracking system," *Appl. Sci.*, vol. 8, no. 1, p. 36, Dec. 2017. [Online]. Available: https://www.mdpi.com/2076-3417/8/1/36

[16] X. Sheng, Y. Chen, L. Guo, J. Yin, and X. Han, "Multitarget tracking algorithm using multiple GMPHD filter data fusion for sonar networks," *Sensors*, vol. 18, no. 10, p. 3193, 2018. [Online]. Available: https://www.mdpi.com/1424-8220/18/10/3193

[17] J. L. Williams, "Marginal multi-Bernoulli filters: RFS derivation of MHT, JIPDA, and association-based member," *IEEE Trans. Aerosp. Electron. Syst.*, vol. 51, no. 3, pp. 1664–1687, Jul. 2015.

[18] J. Smith, F. Particke, M. Hiller, and J. Thielecke, "Systematic analysis of the PMBM, PHD, JPDA and GNN multi-target tracking filters," in *Proc. 22nd Int. Conf. Inf. Fusion*, Jul. 2019, pp. 1–8.

[19] K. Granstrom, L. Svensson, Y. Xia, J. Williams, and A. F. Garcia-Femandez, "Poisson multi-Bernoulli mixture trackers: Continuity through random finite sets of trajectories," in *Proc. 21st Int. Conf. Inf. Fusion (FUSION)*, Jul. 2018, pp. 973–981.

[20] Y. Xia, K. Granstrom, L. Svensson, and A. F. Garcia-Fernandez, "An implementation of the Poisson multi-Bernoulli mixture trajectory filter via dual decomposition," in *Proc. 21st Int. Conf. Inf. Fusion (FUSION)*, Jul. 2018, pp. 1–8.

[21] M. Karataş, "A multi foci closed curve: Cassini oval, its properties and applications," *Doğuş Üniversitesi Dergisi*, vol. 2, no. 14, pp. 231–248, Jul. 2013.

[22] E. Delande, M. Üney, J. Houssineau, and D. Clark, "Regional variance for multi-object filtering," *IEEE Trans. Signal Process.*, vol. 62, no. 13, pp. 3415–3428, Jul. 2014.

[23] Á. F. García-Fernández, J. L. Williams, K. Granström, and L. Svensson, "Poisson multi-Bernoulli mixture filter: Direct derivation and implementation," *IEEE Trans. Aerosp. Electron. Syst.*, vol. 54, no. 4, pp. 1883–1901, Aug. 2018.

[24] G. de Magistris, P. Stinco, J. R. Bates, J. M. Topple, G. Canepa, G. Ferri, A. Tesei, and K. le Page, "Automatic object classification for low-frequency active sonar using convolutional neural networks," in *Proc. OCEANS MTS/IEEE SEATTLE*, Oct. 2019, pp. 1–6.

[25] K. Granström, L. Svensson, Y. Xia, J. Williams, and Á. F. García-Fernández, "Poisson multi-Bernoulli mixtures for sets of trajectories," 2019, *arXiv:1912.08718*.

[26] Y. Xia, K. Granstrom, L. Svensson, A. F. García-Fernández, and J. L. Williams, "Extended target Poisson multi-Bernoulli mixture trackers based on sets of trajectories," in *Proc. 22nd Int. Conf. Inf. Fusion*, Jul. 2019, pp. 1–8.

[27] K. Granstrom, L. Svensson, Y. Xia, A. F. Garcia-Femandez, and J. Williams, "Spatiotemporal constraints for sets of trajectories with applications to PMBM densities," in *Proc. IEEE 23rd Int. Conf. Inf. Fusion (FUSION)*, Jul. 2020, pp. 1–8.

[28] K. G. Murty, "Letter to the editor—An algorithm for ranking all the assignments in order of increasing cost," *Oper. Res.*, vol. 16, no. 3, pp. 682–687, Jun. 1968.

[29] B. Ristic, D. Clark, B.-N. Vo, and B.-T. Vo, "Adaptive target birth intensity for PHD and CPHD filters," *IEEE Trans. Aerosp. Electron. Syst.*, vol. 48, no. 2, pp. 1656–1668, Apr. 2012.

[30] M. Fewell and S. Ozols, "Simple detection-performance analysis of multistatic sonar for anti-submarine warfare," DSTO Defence Sci. Technol. Organisation, SA, Australia, Tech. Rep. DSTO-TR-2562, 2011.

[31] E. Craparo, M. Karataş, and T. U. Kuhn, "Sensor placement in active multistatic sonar networks: Active multistatic sonar networks," *Nav. Res. Logist.*, vol. 64, no. 4, pp. 287–304, Jun. 2017.

[32] R. P. Hodges, *Underwater Acoustics: Analysis, Design and Performance of Sonar*. Hoboken, NJ, USA: Wiley, 2011.

[33] A. R. Fügenschuh, E. M. Craparo, M. Karatas, and S. E. Buttrey, "Solving multistatic sonar location problems with mixed-integer programming," *Optim. Eng.*, vol. 21, no. 1, pp. 273–303, Mar. 2020.

[34] R. P. Hodges, "Design and evaluation of sonars," in *Underwater Acoustics: Analysis, Design and Performance of Sonar*. Hoboken, NJ, USA: Wiley, 2010, pp. 325–337.

[35] B.-T. Vo, B.-N. Vo, and A. Cantoni, "Bayesian filtering with random finite set observations," *IEEE Trans. Signal Process.*, vol. 56, no. 4, pp. 1313–1326, Apr. 2008.

[36] L. Svensson and M. Morelande, "Target tracking based on estimation of sets of trajectories," in *Proc. 17th Int. Conf. Inf. Fusion*, Jul. 2014, pp. 1–8.

[37] A. S. Rahmathullah, A. F. Garcia-Fernandez, and L. Svensson, "Generalized optimal sub-pattern assignment metric," in *Proc. 20th Int. Conf. Inf. Fusion (Fusion)*, Jul. 2017, pp. 1–8.

ERHAN ÖZER was born in Ankara, Turkey, in 1984. He received the Engineering degree from the National Defence University, Istanbul, in 2007, and the M.Sc. degree in acoustic engineering from the Naval Postgraduate School, Monterey, CA, USA, in 2013. He is currently pursuing the Ph.D. degree in electronic engineering. His research interests include underwater multi-target tracking, multistatic sonar, and acoustic signal processing. He received the Outstanding Theses and Dissertations Award by the Naval Postgraduate School, in 2013.

ALI KÖKSAL HOCAOĞLU received the Ph.D. degree in electrical engineering from the University of Missouri-Columbia, USA, in 2000. From 2000 to 2003, he worked as a Postdoctoral Research Associate with the University of Missouri-Columbia and University of Florida, USA. From 2003 to 2012, he worked as the Chief Researcher at the Marmara Research Center and Informatics and Information Security Research Center, Scientific and Technological Research Council of Turkey. He is currently an Assistant Professor with the Department of Electronics Engineering, Gebze Technical University, Turkey. He has worked on a wide variety of applied research problems on automatic target recognition with a focus on problems in pattern recognition, image and signal analysis, and sensor fusion. His current research interests include developing multi-sensor target detection and tracking systems for border surveillance using passive sensors.

• • •